OPTIMUM CURRENT CONTROL FOR A HIGH SPEED AXIAL GAP PERMANENT MAGNET SYNCHRONOUS MOTOR

J. S. Lai, J. M. Bailey
Dept. of Electrical and Computer Engr.
University of Tennessee, Knoxville
Knoxville, Tennessee 37996-2100

R. W. Young, C. W. Sohns, R. A. Hawsey
Technology Applications Center
Oak Ridge National Laboratory
Oak Ridge, Tennessee 37831-7294

Abstract - A high speed (20000 rpm) axial-gap permanent magnet (*PM*) synchronous motor has been constructed and controlled using a new developed algorithm. Due to high speed operation, the implementation using decoupled vector control strategy along with PWM inverter could be difficult and inefficient. In this paper, an optimization algorithm using the Newton-Raphson method is proposed to solve the maximum torque/amp problem for salient-type *PM* motors. The optimum voltage and torque angle for different speeds were further derived from optimum dq-axes currents so that decoupled control can be applied to a 6-step inverter. The complete drive system could be implemented using open-loop optimum voltage and torque angle trajectories or closed-loop control with one variable controlled by a look-up table and the other variable controlled by a closed-loop controller. Both open-loop and closed-loop control systems have been simulated using PC SIMNON, and a closed-loop control system is being fabricated for a 3-phase, 8-pole, 460 V, 27 HP axial-gap *PM* motor. Although torque pulsation cannot be avoided with a 6-step inverter, acceleration is quite smooth due to high load inertia.

1. Introduction

Axial-gap *PM* synchronous machines have several advantages over traditional *PM* machines and induction machines such as high efficiency, high power density (compact size), and wide speed range capability [1,2]. For high speed operation, implementation using decoupled vector control strategy along with a PWM inverter could be difficult and inefficient. The conventional 6-step inverter is thus favored when efficiency and high speed applications are considered.

For high power applications, it is necessary to reduce the current stress of switching devices. A torque/amp maximization using dq-current decoupled vector control has been proposed for interior *PM* machines [3,4]. However, such optimization has not yet been applied to the voltage per Hz (V/Hz) control scheme. In dq-current decoupled vector control, flux is controlled by d-axis current, and torque is controlled by q-axis current. In V/Hz control, flux can be controlled by voltage, and torque can be controlled by torque angle. With voltage and torque angle as the two control variables, decoupling is thus feasible in the V/Hz control scheme.

In this paper, a constant torque acceleration control system using an axial-gap *PM* motor is designed using microcomputer control. The criterion is to accelerate a high inertia load, while overcoming drag losses to 20000 rpm in five minutes or less by developing constant motor torque. . To implement an optimum torque/amp control design by V/Hz control, the voltage and torque angle trajectories are solved and stored in look-up tables for microcomputer control. Optimum voltage and torque angle are derived as a function of different torques and dq-currents. In solving dq-currents for optimum torque/amp ratio, a new algorithm, using the Newton-Raphson iteration method, is developed.

The complete drive system could be implemented using open-loop optimum voltage and torque angle trajectories or closed-loop control with one variable taken from a look-up table and the other variable controlled by a closed-loop PI controller. Both open-loop and closed-loop control systems have been simulated using PC SIMNON, and the closed-loop control system is being fabricated for a 3-phase, 8-pole, 460 V, 27 HP axial-gap *PM* motor. Although the torque pulsation can not be avoided in 6-step inverter, the acceleration is smooth due to high load inertia.

2. Machine Structure and Modeling

The axial gap *PM* motor consists of a thin armature stator winding and a thin rotor disc shown in Figures 1 and 2. Because of low inertia, the disc type machine is suitable for reliable high frequency and high speed operation. The stator is encapsulated in epoxy resin for ruggedness and heat transfer. The saliency of the axial-gap *PM* motor depends highly on air gap width and the number of poles. A smaller air gap and fewer poles will have higher saliency and vice versa.

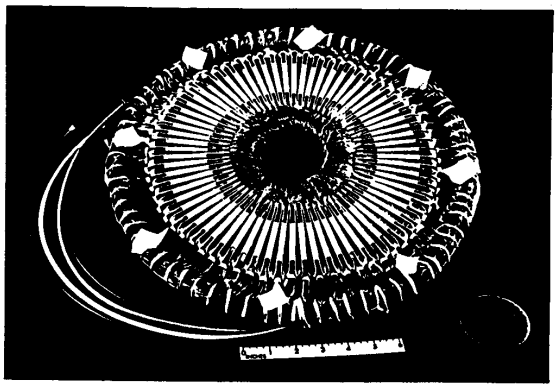

Figure 1: Stator assembly showing teeth and windings prior to encapsulation.

89CH2792-0/89/0000-0767$01.00 © 1989 IEEE

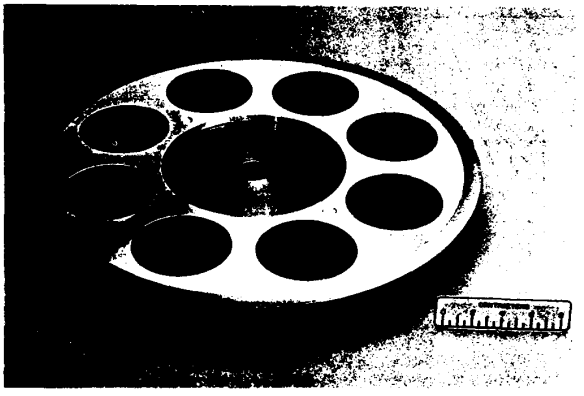

Figure 2: Rotor containing eight Neodymium-iron-boron alloy magnets.

Figure 3 shows the machine model including saliency in synchronously rotating reference frame. The dynamic equation represented by the mathematical model can be derived from the above d-q equivalent circuits. Equation (1) shows the state equations including speed and torque dynamics [5~8]

$$\begin{aligned}
\frac{\mathrm{d}\, i_{qs}}{\mathrm{d}\, t} &= \frac{1}{L_{qs}}(V_{qs} - R_s i_{qs} - \omega_e L_{ds} i_{ds} - E_f) \\
\frac{\mathrm{d}\, i_{ds}}{\mathrm{d}\, t} &= \frac{1}{L_{ds}}(V_{ds} - R_s i_{ds} + \omega_e L_{qs} i_{qs}) \\
\frac{\mathrm{d}\, \omega_r}{\mathrm{d}\, t} &= (T_e - T_L)/J \\
T_e &= \frac{3p}{4}[(L_{ds} - L_{qs}) i_{ds} i_{qs} + \frac{E_f}{\omega_e} i_{qs}]
\end{aligned} \tag{1}$$

where

R_s = stator resistance,

L_{qs} = q-axis inductance,

L_{ds} = d-axis inductance,

E_f = counter EMF,

ω_e = operating frequency,

V_{qs} = q-axis voltage component,

V_{ds} = d-axis voltage component,

i_{qs} = q-axis current component,

i_{ds} = d-axis current component,

ω_r = rotor angular frequency,

T_e = generated torque,

T_L = load torque,

J = inertia, and

p = pole number.

In steady-state, $\mathrm{d}i/\mathrm{d}t = 0$, and the equivalent circuit can be simplified without dynamic quantities. The voltage balance equation can then be represented by (2).

$$\begin{aligned}
V_{ds} &= i_{ds} R_s - i_{qs} \omega_e L_{qs} \\
V_{qs} &= E_f + i_{qs} R_s + i_{ds} \omega_e L_{ds}
\end{aligned} \tag{2}$$

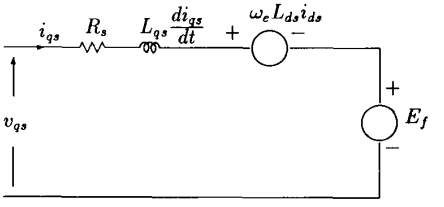

(a) q-axis equivalent circuit

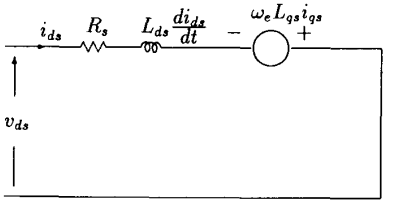

(b) d-axis equivalent circuit

Figure 3: d-q equivalent circuits in synchronously rotating reference frame.

3. Optimum Torque/Amp Control

For surface mounted *PM* machines, an efficiency optimization has been proposed to minimize losses using optimum voltage trajectory as a function of operating frequency [9,10]. This control does not use torque angle as a control variable and is, therefore, typical scalar control.

In vector control, an optimum torque/amp method for the interior permanent magnet *(IPM)* machine has been proposed and applied in traction control [3,4]. In fact, this scheme minimizes stator current for a specific torque. The major advantages of reducing stator current are the lessening of the stress of inverter switching devices and increasing efficiency. The fundamental idea of minimizing stator current can be seen from (1) where torque is a function of dq-axes currents. By varying i_{qs} and i_{ds} for a given torque, a minimum current trajectory can be searched for and found from the whole family of dq current plots [3,4]. This search is required for each given torque and is tedious when finding a set of torque values.

This paper proposes a numerical optimization approach to solve the minimum current trajectory problem, which, indeed, saves a lot of computation time. The optimization is formulated by the following algorithm.

3.1 The Optimization Algorithm

The minimum current problem is posed as

$$\min\ i_s^2(i_{ds}, i_{qs})$$

such that

$$T_e(i_{ds}, i_{qs}) = T_e^*$$

where

$i_s^2 = i_{ds}^2 + i_{qs}^2$, and
T_e^* = a given torque value.

The algorithm to solve the above minimization problem is derived by the following procedure.

1. Eliminate one current variable from the torque equation in (1), i. e.,

$$i_{qs} = \frac{T_e^*}{\frac{3p}{4}[i_{ds}(L_{ds} - L_{qs}) + \psi_f]} \tag{3}$$

where $\psi_f = \frac{E_f}{\omega_e}$.

2. Find the derivative of i_s^2 with respect to i_{ds}.

$$f = \frac{\mathrm{d}(i_s^2)}{\mathrm{d}\, i_{ds}} = 2i_{ds} - \frac{2(T_e^*)^2(L_{ds} - L_{qs})}{(\frac{3p}{4})^2[(L_{ds} - L_{qs})i_{ds} + \psi_f]^3} \tag{4}$$

3. Find the second derivative of i_s^2 with respect to i_{ds}.

$$f' = \frac{\mathrm{d}\, f}{\mathrm{d}\, i_{ds}} = 2 + \frac{6(T_e^*)^2(L_{ds} - L_{qs})^2}{(\frac{3p}{4})^2[(L_{ds} - L_{qs})i_{ds} + \psi_f]^4} \tag{5}$$

4. Apply the Newton-Raphson iteration method to solve i_{ds} such that $f = 0$. The iteration equation is given by

$$i_{ds}(n+1) = i_{ds}(n) - \frac{f(n)}{f'(n)}, \quad n \geq 0. \tag{6}$$

The above algorithm has been applied to an axial-gap *PM* motor. The motor parameters are shown in Table 1.

Table 1: Parameters of an axial-gap *PM* motor.

Rated voltage	460 rms $V_{\ell-\ell}$
Rated speed	20000 rpm
Pole	8
Stator resistance R_s	0.4 Ω
d-axis reactance X_{ds}	5.352 Ω @ 20000 rpm
q-axis reactance X_{qs}	7.240 Ω @ 20000 rpm
Counter EMF E_f	278 V_{peak} @ 20000 rpm

With a reasonable initial guess, most results converged in less than three iterations. Optimum *dq*-axes currents with respect to different torques are plotted in Figure 4.

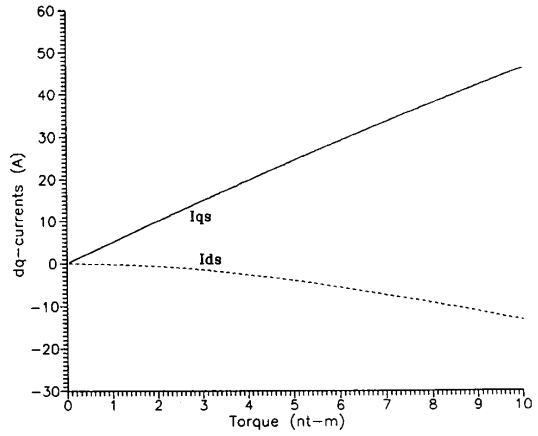

Figure 4: Optimized *dq*-axes currents with respect to different torques.

3.2 Optimization for V/Hz Control

A similar algorithm can also be applied to the V/Hz control method. Since *dq*-axes currents are functions of voltage and torque angle, the torque expression can be formulated using voltage and torque angle. Representing stator phase voltages by (7), the peak voltage $\hat{V}_s$ and torque angle δ can be obtained by the *dq*-transformation [11].

$$\begin{aligned} V_{as} &= \hat{V}_s \cos(\omega_e t + \delta) \\ V_{bs} &= \hat{V}_s \cos(\omega_e t - 120° + \delta) \\ V_{cs} &= \hat{V}_s \cos(\omega_e t + 120° + \delta) \end{aligned} \tag{7}$$

where

$$\begin{aligned} \hat{V}_s &= \sqrt{V_{ds}^2 + V_{qs}^2} \\ \delta &= \tan^{-1} \frac{-v_{ds}}{v_{qs}} \end{aligned} \tag{8}$$

Using the steady-state voltage balance equation (2), voltage and torque angle can be represented as functions of *dq*-axes currents.

$$\begin{aligned} \hat{V}_s &= \sqrt{(E_f + R_s i_{qs} + \omega_e L_{ds} i_{ds})^2 + (\omega_e L_{qs} i_{qs} - R_s i_{ds})^2} \\ \delta &= \tan^{-1} \frac{\omega_e L_{qs} i_{qs} - R_s i_{ds}}{E_f + R_s i_{qs} + \omega_e L_{ds} i_{ds}} \end{aligned} \tag{9}$$

According to (9), a simple decoupling which relates $\hat{V}_s/\omega_e$ to i_{ds} and δ to i_{qs} is possible provided that $R_s = 0$ and $L_{qs} = L_{ds}$. If $R_s \neq 0$ and $L_{qs} \neq L_{ds}$, the above relationship will not be simple. However, optimized trajectories of $\hat{V}_s$ and δ can be plotted using Figure 4 and (9). Optimized phase voltage $\hat{V}_s$ and torque angle δ trajectories are plotted in Figure 5 and Figure 6, respectively.

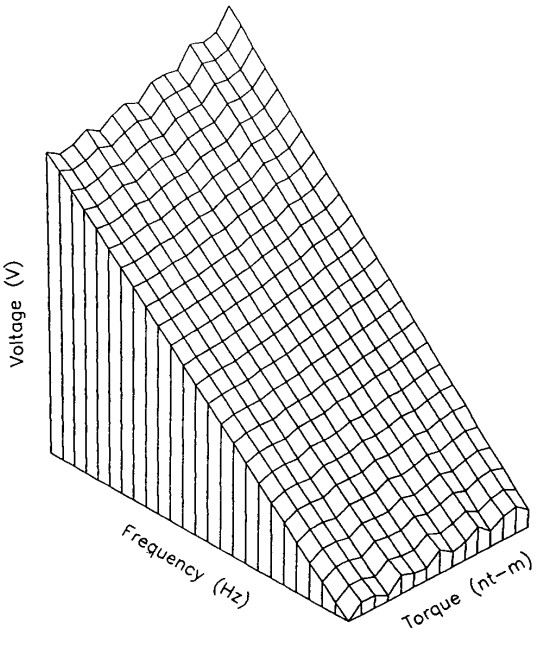

Figure 5: Optimized phase voltage $\hat{V}_s$ trajectory with respect to torque and frequency.

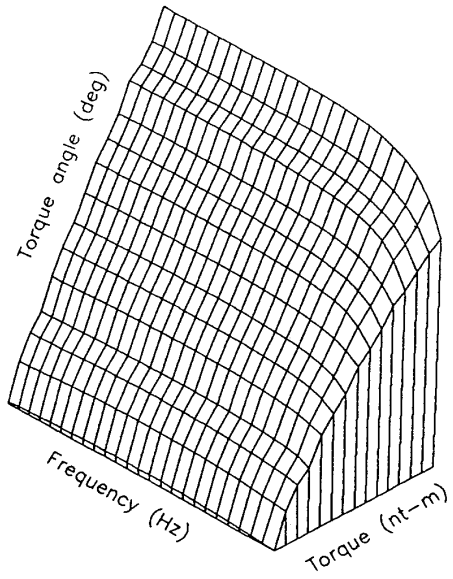

Figure 6: Optimized torque angle δ trajectory with respect to torque and frequency.

From Figure 5, it can be seen that the voltage as function of frequency is almost linear. Thus, in actual microcomputer implementation, the voltage $\hat{V}_s$ can be easily calculated using a linear relationship with respect to frequency, and δ values can be stored in a ROM look-up table or controlled by a closed-loop controller.

4. Control of an Axial-Gap *PM* Motor

The speed of a synchronous machine is uniquely determined by the supply frequency. Thus, speed can be easily controlled by an open loop voltage/Hz inverter. To control flux, the voltage command V_s^* of the DC chopper is controlled by the frequency command ω_r^*. Constant torque can be controlled by a firing delay angle α which is a function of torque angle δ and the signal conditioning circuit delay of the position sensor. The control of a *PM* motor is thus decoupled like that of a DC machine. Figure 7 shows an open loop voltage/Hz control system using optimization results.

In order to have reliable current control, the delay control angle α_d^* has to be controlled by a phase-locked loop (PLL) circuit. Although the voltage command V_s can be controlled by the analytical results, a closed-loop control system is preferable because parameter variation and the saturation effect were not considered in mathematical analysis. Figure 8 shows a closed-loop current control system. The reference voltage signal V_s is controlled by a *PI* controller in order to eliminate steady-state error and to maintain constant DC link current and constant torque.

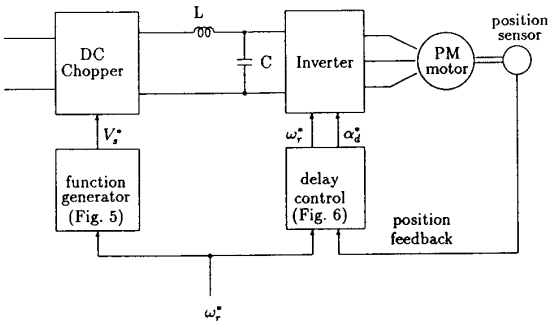

Figure 7: Open-loop V/Hz control system of an axial-gap *PM* motor.

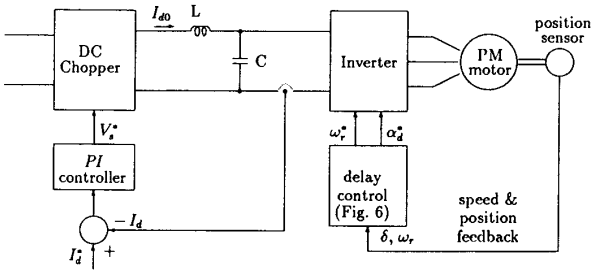

Figure 8: Closed-loop V/Hz control system of an axial-gap *PM* motor.

5. Simulation of Constant Torque Acceleration

The systems of Figures 7 and 8 were simulated using PC SIMNON. Although a six-step inverter is used here, a PWM type inverter could be a candidate provided that high power high switching speed devices are available and drive performance is the main consideration and not efficiency.

Most system parameters are not constant. The typical load inertia is 0.5 slug-ft^2, and the worst case is 0.625 slug-ft^2. The worst case drag torque T_L (ft-lb) can be expressed as a function of speed N (rpm), i.e.,

$$T_L = 0.06667 + 2.117 \times 10^{-5} N + 9.8082 \times 10^{-9} N^2 + 7.3448 \times 10^{-14} N^3.$$

The control criterion is to increase speed from zero to 20000 rpm in 5 minutes or less by constant motor torque. In order to determine how much generated torque is required, the acceleration profiles for different load torques were studied as shown in Figure 9.

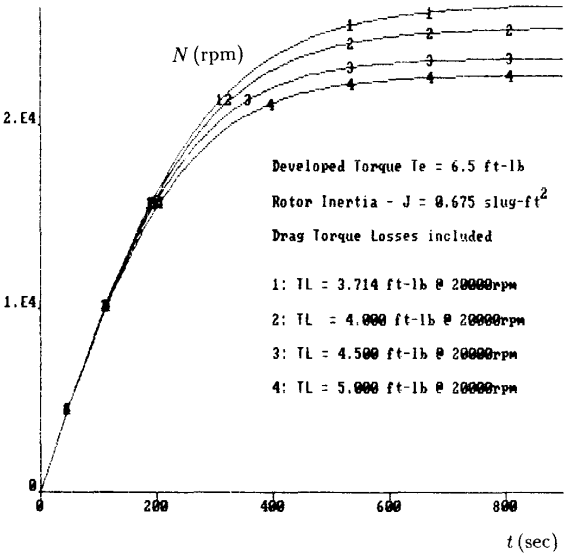

Figure 9: Acceleration profiles of a high speed axial-gap *PM* motor.

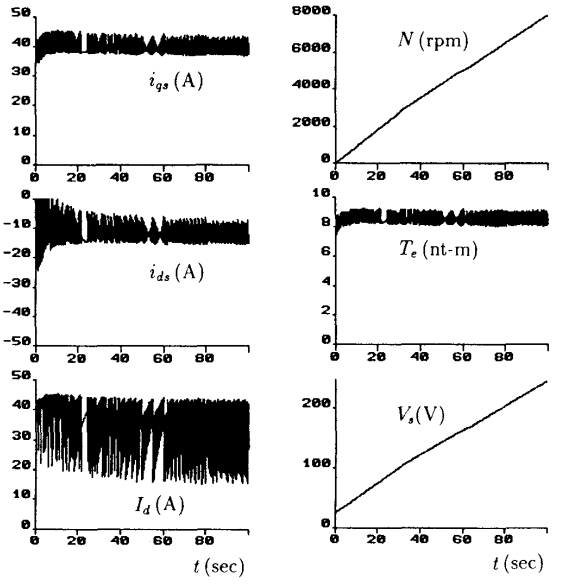

Figure 10: Open-loop V/Hz control system simulation results.

Notice that the worst case inertia (motor rotor plus load) is 0.675 slug-ft^2. The result shows that a torque command of 8.8 nt-m (6.5 ft-lb) will satisfy the performance requirement for a worst case drag torque of 5 ft-lb at 20000 rpm. This torque command was first translated to current commands as indicated in Figure 4, and then converted to optimum voltage and torque angle commands as shown in Figures 5 and 6.

The complete system including DC voltage regulator, DC link LC filter, 6-step inverter, and *PM* motor was simulated for open-loop and closed-loop systems. Using torque command $T_e^* = 8.8$ nt-m, the simulation results are shown in Figures 10 and 11.

For the open-loop control system, the voltage command V_s^* was approximated by a first order equation, and the firing delay angle command α_d^* was found from a look-up table. According to Figure 10, the decoupled control using voltage and torque angle as control variables effectively yields constant dq currents i_{ds} and i_{qs}. The generated torque T_e thus remains constant during acceleration.

For the closed-loop control system, a low gain PI regulator was used for better stability. However, the system response was quite slow. This gain, of course, is adjustable and can be varied to obtain the best response. The DC link circuit has an LC filter between the DC chopper and the inverter. The inverter side current I_d is noisy, but the DC supply side current I_{d0} is quite clean.

The main problem with using a six-step inverter is torque pulsation caused by switching. This can be seen from the simulation results. The frequency of the pulsating torque is six times the fundamental supply frequency. However, for high inertia load, acceleration remains smooth.

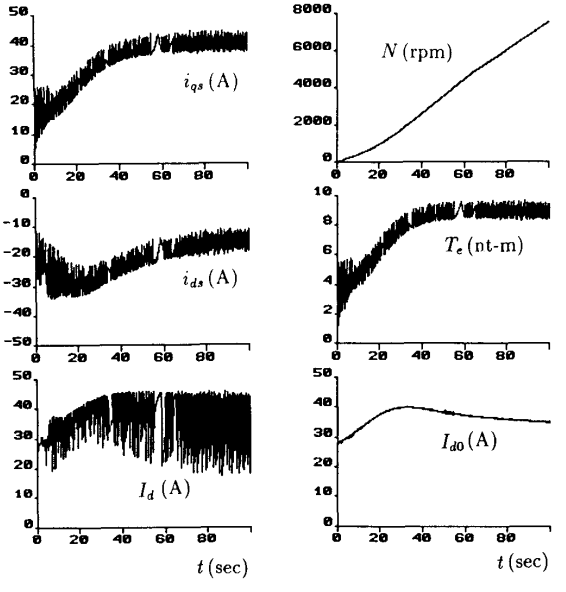

Figure 11: Closed-loop V/Hz control system simulation results.

6. Conclusion

An axial-gap *PM* motor is modelled for a salient type *PM* motor. The maximum torque/amp problem for this class machine is solved by the proposed algorithm using the Newton-Raphson method. For high speed operation, the optimization of torque/amp is extended to 6-step type inverters. Decoupling for V/Hz control is feasible by manipulating voltage and torque angle simultaneously. Simulation shows satisfactory results for both open-loop and closed-loop systems.

References

[1] J. M. Bailey, R. A. Hawsey, C. W. Sohns, R. N. Nodine, and G. R. Boser, "A Self-Starting, Axial-Gap Permanent Magnet Motor and Adjustable-Speed Drive," *Proceeding of 1988 IEEE Southeast Conference*, pp. 518–522, 1988.

[2] R. A. Hawsey, J. M. Bailey, C. W. Sohns, C. E. Leonard and C. P. White, *Performance Test Results: Axial-Gap Permanent Magnet Compressor Motor*, Martin Marietta Record, No. K/ETAC-51, Feb, 1988.

[3] T. M. Jahns, G. B. Kliman, and T. W, Noumann, "Interior Permanent Magnet Synchronous Motors for Adjustable-Speed Drives," *Conference Record of IEEE IAS Annual Meeting*, pp. 814–823, 1985.

[4] T. M. Jahns, "Flux-Weakening Regime Operation of an Interior Permanent Magnet Synchronous Motor Drive," *Conference Record of IEEE IAS Annual Meeting*, pp. 814–823, 1986.

[5] B. K. Bose, "A High Performance Inverter-Fed Drive System of an Interior Permanent Magnet Synchronous Machine," *Conference Record of IEEE IAS Annual Meeting*, pp. 269–276, 1987.

[6] B. K. Bose and P. M. Szczesny, "A Microcomputer-Based Control and Simulation of an Advanced IPM Synchronous Machine Drive System for Electric Vehicle Propulsion," *Conference Record of IEEE IECON '87*, pp. 454–463, 1987.

[7] M. A. Rahman, T. A. Little, and G. R. Slemon, "Analytical Models for Interior-tpye Permanent Magnet Synchronous Motors," *IEEE Trans. on Magnets*, Vol. MAG-21, No. 5, pp. 1741–1743, Sept. 1985.

[8] M. A. Rahman, "High Efficiency Permanent Magnet Synchronous Motors," *Conference Record of IEEE IAS Annual Meeting*, pp. 561–564, 1979.

[9] R. S. Colby and D. W. Novotny, "Efficient Operation of Surface Mounted PM Synchronous Motors," *IEEE Trans. on Industry Applications*, Vol. IA-23, No. 6, pp. 1048–1054, Nov./Dec. 1987.

[10] R. S. Colby and D. W. Novotny, "An Efficiency-Optimizing Permanent-Magnet Synchronous Motors," *IEEE Trans. on Industry Applications*, Vol. IA-24, No. 3, pp. 462–469, May/June 1988.

[11] R. H. Park, "Two-Reaction Theory of Synchronous Machines - I," AIEE Trans., Vol. 48, pp. 716-721, June 1920.